An investigation of trace and isotope light elements in mineral phases from well RN-17 (Reykjanes Peninsula, SW Iceland)

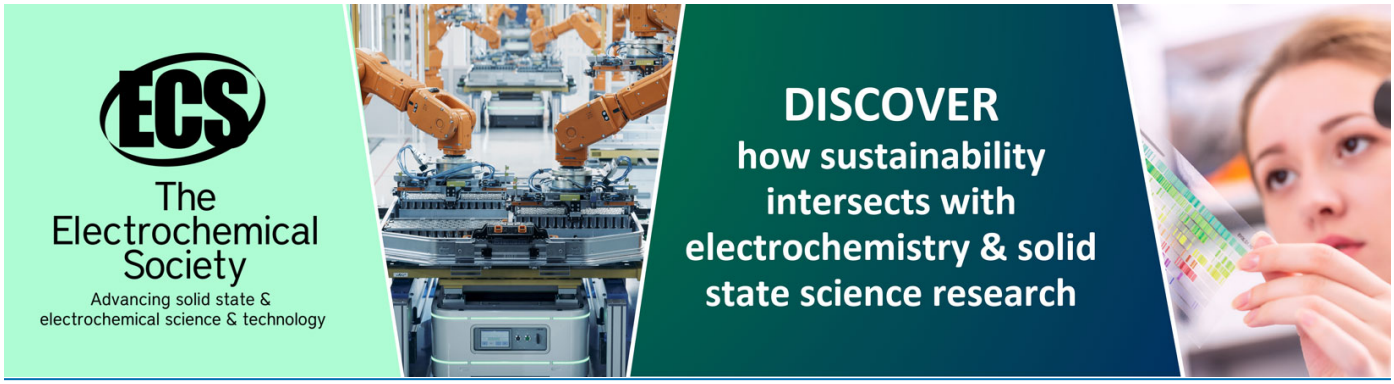

IOP Conf. Series: Materials Science and Engineering **7** (2010) 012026 doi:10.1088/1757-899X/7/1/012026

An investigation of trace and isotope light elements in mineral phases from well RN-17 (Reykjanes Peninsula, SW Iceland)

N Raffone[1,5], L P Ottolini[1], S Tonarini[2], G Gianelli[2], M D'Orazio[3] and G Ó Fridleifsson[4]

[1] Consiglio Nazionale delle Ricerche, Istituto di Geoscienze e Georisorse (IGG), Sezione di Pavia, via Ferrata 1, IT-27100 Pavia, Italy
[2] Consiglio Nazionale delle Ricerche, Istituto di Geoscienze e Georisorse (IGG), Sezione di Pisa, via Moruzzi 1, IT-56124 Pisa, Italy
[3] Università di Pisa, Dipartimento di Scienze della Terra, via S. Maria 53, IT-56126 Pisa, Italy
[4] Hitaveita Sudurnesja Ltd., Brekkkustigur 36, IS-260 Reykjanesbaer, Iceland

E-mail: raffone@crystal.unipv.it

Abstract. The light lithophile (Li, Be and B) and halogen (F, Cl) elements are powerful tracers of fluid transfer due to their mobility during high temperature hydrothermal processes and metamorphic devolatilisation. Moreover, although a great deal of studies have been carried out on these elements in whole rock and minerals of altered rocks from divergent and convergent plate margins, an inventory for mineral phases from the altered Icelandic oceanic crust is still incomplete.
In the present paper we report the results of in situ EPMA and SIMS investigations on variously altered magmatic (plagioclase and clinopyroxene) and hydrothermal phases (amphibole and epidote) from selected cuttings drilled at different depths (400 - 3000 m) of the well RN-17, Reykjanes geothermal system (SW Iceland). Our study has benefited from the use of high-magnification SEM investigations; from ICP-MS on Li, P-TIMS determinations of boron isotope composition ($\delta^{11}B$) and ID analyses of B contents on the whole rock.
Particularly, SIMS data on epidote have shown that alteration beneath Reykjanes has been more efficient in the shallow and intermediate cuttings, while whole rock data on boron isotope composition have revealed that the alteration has been caused firstly by $\delta^{11}B$-poor fluids and successively by $\delta^{11}B$-rich seawater-hydrothermal fluids.

1. Introduction

The geochemical study of the mineral phases of volcanic rocks from Reykjanes Peninsula, the landward extension of the Reykjanes Ridge (figure 1), is necessary in order to determine constitutive rock properties, understand the nature and formation of rock permeability, and constrain the alteration processes occurring [1]. The achievement of these targets represents the main purpose of the Iceland Deep Drilling Project (IDDP), which is to find out if the accessible part of the geothermal resource base can be enlarged significantly at the expense of the inaccessible part, in order to increase useful and economic exploitation of geothermal energy [2]. In this frame, we carried out [3] secondary ion

[5] To whom any correspondence should be addressed.

mass spectrometry (SIMS) investigations of Li, B and Cl in clinopyroxene (cpx), plagioclase (plg) and amphibole (amph), along with inductively coupled plasma mass spectrometry (ICP-MS) and isotope dilution (ID) analyses on the whole rock Li and B contents in selected samples, i.e., three drill-cuttings (RN-17-1100, -2150, -3000), one unaltered lava (RN-17-GIOV-2), and one core-sample (dolerite dyke RN-19-2246) from wells RN-17 and RN-19, both located in the Reykjanes high-temperature hydrothermal system, SW Iceland (figure 1). The main results were the following: i) the comparison of Li and B whole rock data with those from literature showed that our samples are affected by seawater hydrothermal alteration; ii) in the most B-enriched cutting RN-17-2150 a positive correlation occurred between B whole rock and Cl-contents in the mineral phases; iii) amphibole seemed to be the main host phase for chlorine; and iv) fracture zones occurring in mineral phases were responsible for local Cl enrichment. As for B, however, we observed a discrepancy between the B-content in the whole rock and the B budget in the mineral phases, thus suggesting a major partitioning of boron in hydrothermally-related secondary phases, such as epidote.

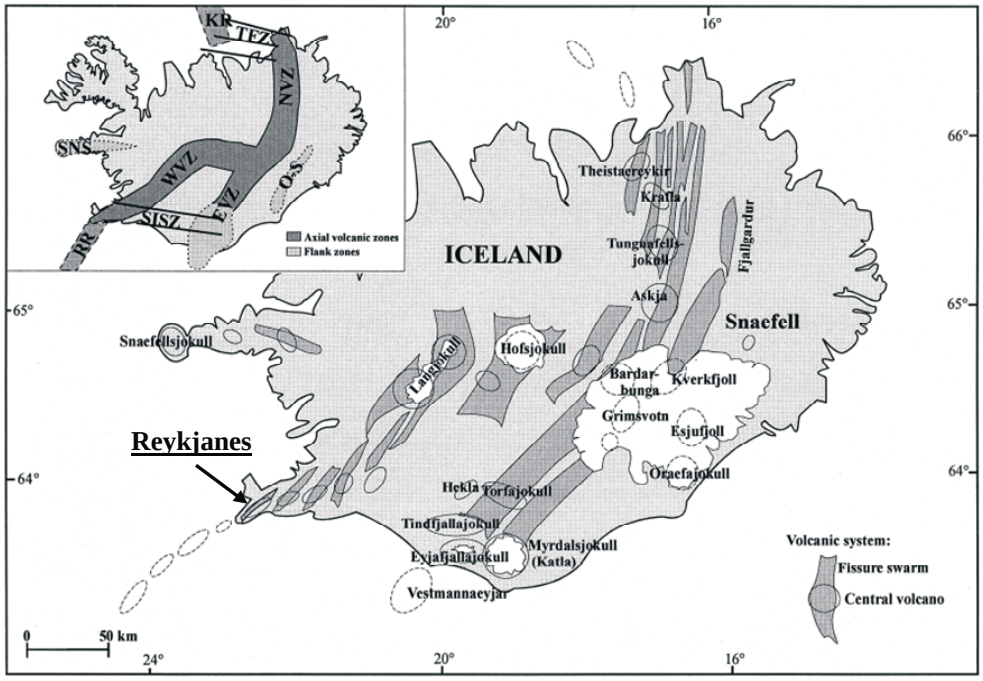

Figure 1. Schematic geologic map of Iceland showing the major tectonic and volcanic features, and the location of the Reykjanes geothermal system [25]. In the inset: RR = Reykjanes Ridge, SISZ = South Iceland seismic zone, WVZ = Western volcanic zone, NVZ = Northern volcanic zone, EVZ = Eastern volcanic zone, TFZ = Tjornes fracture zone, KR = Kolbeinsey ridge, SNS = Snæfellsnes volcanic zone, O-S = Öræfajökull-Snæfell zone.

The aim of the present work is to study at the ion microprobe the Li-, B-, Be- and F-contents on epidote (ep) and amphibole (amph), and to increase the SIMS data set for some elements (Li, B) in clinopyroxene and plagioclase of 9 basaltic drill-cuttings, selected on the basis of different depths (400 - 3000 m), and one core-sample from the above reported two wells. The microanalytical study here described, the first in literature for this area, along with additional data on whole rock B-content, by means of isotope dilution, and boron isotope composition ($\delta^{11}B$) is essential to effectively characterize the geochemical processes occurring at depth within Reykjanes geothermal system; that

is: i) to understand the partitioning of volatile elements among different mineral phases; ii) to investigate the relationship occurring between seawater-alteration degree and the drilled depth; and iii) to gain insight into the nature of the supercritical fluids occurring within the oceanic crust beneath the Reykjanes Peninsula.

The decision of studying epidote stems from the fact that it is an indicator of the temperature regime in hydrothermal systems ([4] and references therein) and it has the property to incorporate boron, which represents one of the more mobile elements and more sensitive tracers of water-rock interactions [5].

2. Geologic background

The Reykjanes high-temperature hydrothermal system, placed within a rift system in which the Reykjanes Ridge portion of the Mid Atlantic Ridge comes on land, represents the westernmost and one of the smallest high temperature areas in Iceland, with surface thermal activity covering only about 1 km^2 (figure 1). Differently from other high-temperature systems, Reykjanes is characterized by the persistence of basaltic rock-permeability at depth, due to the paucity of impermeable-intrusive rocks between 1 - 2 km depth [6]. This is the most important feature as the permeability is the key physical parameter controlling the mechanisms of water/rock interaction and the evolution of submarine alteration [7]. This peculiarity makes the Reykjanes site an ideal setting for research on supercritical fluids in Iceland.

3. Sample description

The mineral phases selected for the SIMS study are from 9 basaltic drill-cuttings (RN-17-650, -750, -1100, -1450, -1550, -1700, -2150, -2800, -3000), and one dolerite dyke (RN-19-2246). Owing to the characteristics of the available cuttings in the form of granulate materials, selected mineral phases were embedded in epoxy-resin mounts. Such mounts are the same on which we already performed major, minor and trace investigations [8]. Whole rock B-contents were investigated on 10 drill-cuttings (RN-17-400, -650, -750, -1100, -1450, -1550, -1700, -2150, -2800, -3000), on a dolerite dyke (RN-19-2246), and on the surface lava RN-17-GIOV-2, while boron isotope composition was analyzed on 8 drill-cuttings (RN-17-400, -650, -750, -1100, -1450, -1550, -2150, -3000), and on GIOV-2 lava. Petrographic evidence of the studied samples comes from stratigraphy of well RN-17 included in [6].

4. Analytical technique

Whole rock B and $\delta^{11}B$ were determined using a VG Isomass 54E positive ion thermal ionisation mass spectrometer (P-TIMS) at CNR-IGG, Pisa.

Boron concentrations were determined by isotope dilution using alkaline fusion with K_2CO_3 followed by three steps of ion exchange purification ([9] and references therein). Analytical uncertainty on elemental analysis is estimated to be ± 5 % on the basis of replicate analyses of Glass Standard Material Japanese Basalt (GSM JB-2) (average boron concentration of 28.8 ± 0.9 $\mu g.g^{-1}$, recommended value 30 $\mu g.g^{-1}$); and Rhyolite USGS Standard (RGM-1) (average B value of 27.8 ± 0.8 $\mu g.g^{-1}$, recommended value 28 $\mu g.g^{-1}$). This conservative error is ascribed almost entirely to the alkaline fusion of the samples before adding the spike solution (NIST SRM 952); replicate analyses of the same solution agree within 0.2 %.

Boron isotope composition was determined after B extraction and the purification procedure described by [9]. Accuracy of the procedure was evaluated by repeated analyses of NIST-SRM 951 standard taken through the full chemistry procedure and by replicate analyses of GSM JB-2 basalt reference standard. Isotopic fractionation associated with the mass-spectrometer analysis was corrected using a fractionation factor calculated as $[(R_{cert} + 0.00079) / R_{meas}]$; $^{11}B/^{10}B_{meas}$ (NIST 951) = 4.0525 ± 0.0010 (2σ) and $^{11}B/^{10}B_{meas}$ (JB-2) = 4.0820 ± 0.0014 (2σ). Boron isotopic compositions of the samples are reported in the conventional delta notation ($\delta^{11}B$) as per mil deviation from accepted composition of NIST-SRM 951 (certified $^{11}B/^{10}B$ = 4.04362; [10]).

Whole-rock Li was obtained by ICP-MS (Fisons PQ2 Plus®) at Dipartimento di Scienze della Terra, Università di Pisa. Analytical precisions, evaluated by repeated analyses of the in-house standard HE-1 (Mt. Etna hawaiite), is generally between 2 and 5 % RSD, whereas for unknown samples with low Li content the error is about 10 %. Detection limits for Li at the 3σ-level are 0.05 $\mu g.l^{-1}$ [11]. Concentration of Li ($\mu g.g^{-1}$) in four international geochemical reference samples determined along with the unknown samples of this work yielded: BIR-1 = 3.2 - 3.3 $\mu g.g^{-1}$ (reference value 3.4 $\mu g.g^{-1}$); WE-E = 14.1 - 14.7 $\mu g.g^{-1}$ (reference value 13.6 $\mu g.g^{-1}$); PM-S = 7.6 $\mu g.g^{-1}$ (reference value 7.3 $\mu g.g^{-1}$); and OU-6 = 99 - 103 $\mu g.g^{-1}$ (reference value 95 $\mu g.g^{-1}$).

The selected mineral grains were analyzed for major and minor elements with a Jeol 8200 Super Probe (Dipartimento di Scienze della Terra, Università di Milano), according to electron probe microanalysis (EPMA), using a beam current of 15 nA and acceleration voltage of 15 kV. Standard description and detailed analytical conditions are reported in [8].

The SIMS investigations, performed on the same mineral crystals, were carried out with a Cameca IMS 4f ion microprobe installed at CNR-IGG (Pavia), bombarded with a $^{16}O^-$ primary beam of 10 nA current intensity that was focused onto a micro-spot area of ~ 15 µm in diameter. The width of the energy slit was 50 eV and the voltage offset applied to the sample accelerating voltage (+4.5 kV) was -100 V. Positive filtered secondary ions were extracted and focused under an ion image field of 25 µm. We used the largest contrast diaphragm and field aperture (400 and 1800 µm Ø, respectively), at a mass resolving power of ~ 900 (M/ΔM). We measured the following isotopes $^7Li^+$, $^9Be^+$, $^{11}B^+$ and $^{19}F^+$. $^{30}Si^+$ was selected as the isotope of the reference element (Si) for these matrixes. Counting times were: 20 sec for Li and Be (each), 40 sec for B and F (each), and 8 sec for Si over four analytical cycles, after about 8 min waiting time necessary to achieve steady-state sputtering conditions. Conversion of ion intensities into concentrations was empirically accomplished by measuring the ion yield relative to Si of each element in reference samples. The mineral grains after ion probe investigations were re-analyzed with the electron microprobe at the same SIMS spots, and the relative silica contents were used in the final SIMS quantification procedures. Concentrations of Li, Be, B and F were obtained by means of our calibration curves for silicates [12, 13]. International standards, i.e., NIST-SRM 610, 612 and 614, in addition to a CNR-IGG internal standard, i.e., kaersutite Soda Springs (KSS) were used in the calibration procedure. Accuracy and precision are in the range 5 - 10 % rel. for Li, Be and B, and typically ~ 15 % for F.

5. Analytical results and discussion

SIMS data (in ppm) (Table 1) show that: i) Li: 0.28 - 5.38 in clinopyroxene (cpx), 0.02 - 0.32 in plagioclase (plg), 0.55 - 2.3 in amphibole (amph), 0.01 - 0.32 in epidote (figures 2a, b, c, d); ii) B: 0.02 - 0.50 in cpx, 0.01 - 0.90 in plg, 0.14 - 2.3 in amph, 0.60 - 8.9 in epidote (figures 3a, b, c, d); and iii) F: 16 - 174 in cpx, 4 - 7 in plg, 4.2 - 574 in amph, 4.2 - 110 in epidote, are characterized by preferential mineral phase partitioning with cpx the main host phase for Li, epidote for B, and amphibole for fluorine. This behaviour is less marked for Be (0.01 - 1.3 in epidote, 0.47 - 3.1 in amph, 0.01 - 0.38 in cpx, 0.09 - 1.8 in plg), showing amph and plg to be the main host phases for this element. In addition, the SIMS data on cpx and epidote have shown that the B-contents in epidote and those for Li in cpx are comparable with those of the overall whole rock range (B = 3.3 - 11.4 ppm; Li = 1.9 - 5.7 ppm) obtained by ID and ICP-MS (figures 4 and 5). Figures 4 and 5 also show that whole rock B and Li of our cuttings are characterized by a different behaviour: B-contents are higher than those of fresh MORB (figure 4), whereas Li concentrations are lower than those of basalts from literature (figure 5). This discrepancy is in agreement with the expected higher mobility of B ([3] and references therein) in hydrothermal systems, such as Reykjanes one. The low Li-contents in our basalts can be justified under the hypothesis that hydrothermal fluids lost Li as a consequence of the precipitation of Li-bearing phases (mainly clinopyroxene and amphibole) during early fluid/rock interactions.

As for F, the lack of whole rock concentrations for our cuttings has not allowed to make a direct comparison with literature whole rock F-contents. On the basis of the SIMS data obtained in this

Table 1. Experimental data obtained by SIMS (Li, B on single mineral phases), ICP-MS (WR Li), ID (WR B) and P-TIMS ($\delta^{11}B$) for the studied cuttings of the Reykjanes geothermal field.
SIMS = secondary ion mass spectrometry; ICP-MS = inductively coupled plasma mass spectrometry; ID = isotope dilution; P-TIMS = positive ion thermal ionisation mass-spectrometer; WR = whole rock; cpx = clinopyroxene; plg = plagioclase; ep = epidote; amph = amphibole.

Sample	Rock type	Analytical techniques	Li (ppm)	B (ppm)	Be (ppm)	F (ppm)	$\delta^{11}B$	2σ
RN-17-400 WR	Altered basalt	ID, P-TIMS		6.06			-6.4	*0.7*
RN-17-650 WR		ICP-MS, ID, P-TIMS	5.50	11.38			-4.4	*0.4*
ep-2a		SIMS	0.06	2.43	0.75	27		
ep-2b		SIMS	0.15	3.15	0.75	27		
ep-1a lighter area		SIMS	0.04	2.47	0.17	39		
ep-1b darker area		SIMS	0.16	7.98	0.70	27		
ep-1c lighter area		SIMS	0.08	3.48	0.15	26		
ep-3a lighter area		SIMS	0.07	4.31	0.59	19		
ep-3b lighter area		SIMS	0.17	8.94	0.58	24		
RN-17-750 WR	Altered basalt	ID, P-TIMS		5.51			-7.7	*0.7*
ep-2a darker area		SIMS	0.23	0.24	1.09	25		
RN-17-1100 WR	Altered basalt	ICP-MS, ID, P-TIMS	2.53	6.23			-10.5	*0.6*
cpx-1a		SIMS	0.28	0.11	0.23	36		
cpx-1c		SIMS	1.19	0.03	0.08	16		
cpx-3a		SIMS	1.64	0.04	0.13	24		
cpx-3b		SIMS	1.33	0.02	0.03	29		
cpx-7b		SIMS	1.55	0.241				
cpx-7g		SIMS	1.1	0.208				
plg-1b		SIMS	0.10	0.02	1.78	5.9		
plg-x		SIMS	0.13	0.02	0.78	3.9		
plg-1ay		SIMS	0.11	0.01	0.86	7.2		
plg-1by		SIMS	0.09	0.02	1.04	5.9		
pg-7a		SIMS	0.06	0.099				
pg-7a(2)		SIMS	0.06	0.126				
ep-1a lighter area		SIMS	0.04	1.39	0.72	48		
ep-1b darker area		SIMS	0.06	4.15	0.84	37		
ep-2b darker area		SIMS	0.04	1.18	0.11	27		
ep-3a lighter area		SIMS	0.04	1.43	0.26	21		
ep-3b lighter area		SIMS	0.51	1.84	0.6	22		
RN-17-1450 WR	Altered basalt	ID, P-TIMS		5.29			-9.6	*0.4*
cpx-1a		SIMS	5.38	0.04	0.04	50		
cpx-2a		SIMS	1.55	0.05	0.22	38		
cpx-2b		SIMS	1.69	0.05	0.19	25		
plg-1a		SIMS	0.02	0.03	1.04	4.9		
ep-1a darker area		SIMS	0.21	2.5	0.05	78		
ep-2a darker area		SIMS	0.04	1.51	0.12	31		
ep-2b darker area		SIMS	0.05	3.15	0.12	45		
ep-3a darker area		SIMS	0.04	4.72	0.004	93		
ep-3b darker area		SIMS	0.05	7.1	0.02	96		
ep-3b(2) darker area		SIMS	0.07	8.1	0.01	88		
RN-17-1550 WR	Altered basalt	ID, P-TIMS		7.1			-15.4	*0.5*
cpx-1a		SIMS	1.97	0.04	0.05	49		
cpx-1b		SIMS	3.63	0.05	0.09	53		
cpx-2a		SIMS	3.18	0.07	0.05	57		
plg-2b		SIMS	0.08	0.10	0.22	6		
ep-1a lighter area		SIMS	0.01	0.32	0.11	44		
ep-1b darker area		SIMS	0.03	0.61	0.31	24		
ep-2b darker area		SIMS	0.27	5.2	0.43	110		
ep-3a lighter area		SIMS	0.04	1.99	0.10	27		
ep-3b lighter area		SIMS	0.14	8.4	0.11	74		
RN-17-1700 WR	Altered basalt							
plg-2a		SIMS	0.32	0.02	0.09	6.5		
plg-2b		SIMS	0.25	0.03	0.18	4.2		
ep-1a darker area		SIMS	0.03	0.94	1.29	43		
ep-1b darker area		SIMS	0.02	0.62	0.59	22		
ep-2a darker area		SIMS	0.05	0.55	0.52	31		
ep-2b darker area		SIMS	0.01	0.79	0.68	46		
ep-3a darker area		SIMS	0.01	1.13	0.44	30		
ep-3b darker area		SIMS	0.003	0.93	0.52	34		
ep-4b darker area		SIMS	0.01	0.83	0.35	26		

Table 1. continued.

Sample	Rock type	Analytical techniques	Li (ppm)	B (ppm)	Be (ppm)	F (ppm)	$\delta^{11}B$	2σ
RN-17-2150 WR	Altered basalt	ICP-MS, ID, P-TIMS	3.56	12.38			-9.6	*0.3*
cpx-1a		SIMS	4.01	0.03	0.08	125		
cpx-2a		SIMS	2.82	0.02	0.11	61		
cpx-2b		SIMS	5.02	0.04	0.09	176		
cpx-6b(3)		SIMS	3.22	0.306				
cpx-6b(4)		SIMS	2.37	0.525				
cpx-6b(5)		SIMS	2.84	0.505				
pg-6a		SIMS	0.05	0.083				
pg-6f(2)		SIMS	0.51	0.908				
amph-1a		SIMS	1.55	1.82	1.97	574		
amph-1b		SIMS	1.76	2.34	3	76		
amph-2a		SIMS	2.25	2.28	3.09	91		
ep-1a darker area		SIMS	0.10	3.4	0.14	108		
ep-1b lighter area		SIMS	0.06	3.8	0.39	25		
ep-3a darker area		SIMS	0.06	2.2	0.37	63		
ep-3b darker area		SIMS	0.04	0.89	0.48	19		
RN-17-2800 WR	Altered basalt	ID		3.28				
cpx-1a		SIMS	2.0	0.005	0.12	43		
cpx-1b		SIMS	1.79	0.03	0.01	63		
cpx-2a		SIMS	2.46	0.03	0.07	80		
cpx-2b		SIMS	3.85	0.03	0.08	111		
amph-2b		SIMS	2.07	0.99	0.63	64		
ep-1a darker area		SIMS	0.01	0.53	0.98	30		
ep-1b darker area		SIMS	0.03	0.52	1.13	43		
ep-3a darker area		SIMS	0.02	1.33	0.03	25		
ep-3b darker area		SIMS	0.03	0.92	0.44	28		
ep-3c lighter area		SIMS	0.01	0.98	0.43	32		
RN-17-3000 WR	Altered basalt	ICP-MS, ID, P-TIMS	2.22	9.27			-14.4	*0.5*
cpx-1a		SIMS	0.65	0.02	0.04	48		
cpx-1b		SIMS	0.52	0.02	0.04	48		
cpx-5b		SIMS	4.47	0.628				
cpx-5f		SIMS	3.46	0.288				
cpx-5f(2)		SIMS	3.44	0.277				
pg-5e		SIMS	0.10	0.16				
pg-5m		SIMS	0.06	0.069				
amph-1a		SIMS	0.79	0.79	0.50	73		
amph-1a(2)		SIMS	0.64	0.64	0.47	78		
amph 2a		SIMS	0.55	0.14	1.67	42		
ep-1a darker area		SIMS	0.05	0.93	0.23	23		
ep-1b darker area		SIMS	0.08	0.63	0.31	25		
ep-1c darker area		SIMS	0.07	0.85	0.48	26		
ep-2a darker area		SIMS	0.01	0.94	0.08	14		
ep-2b darker area		SIMS	0.04	1.09	0.23	20		
RN-17-GIOV-2 WR	Surface lava	ICP-MS, ID, P-TIMS	5.66	3.83			-18.3	*0.6*
RN-19-2246 WR	Dolerite dyke	ICP-MS, ID	1.85	2.44				
cpx-2a		SIMS	2.61	0.09	0.01	47		
cpx-2b		SIMS	2.17	0.05	0.02	84		
cpx-3a		SIMS	2.21	0.19	0.29	45		
cpx-3b		SIMS	2.45	0.21	0.38	52		
cpx-2b(2)		SIMS	2.19	0.115				
pg-4a		SIMS	0.14	0.046				
pg-4b		SIMS	0.12	0.053				

study, however, it is to be noted that the F-content in the mineral phases analysed, except for amphibole, is lower or comparable to that of the unaltered picrite (<15 - 61 ppm) and tholeiite (94 - 305 ppm) lavas from the Reykjanes Peninsula [14].

The investigation of epidote by SIMS has considered the occurrence of micro-areas with different chemical composition, i.e., Fe-rich lighter and Al-rich darker ones (as previously observed in [8]), and the fact that these areas have been generally of micron-scale size, that is to say, comparable or smaller than the SIMS spot under the present analytical conditions (figure 6). The SIMS analyses carried out

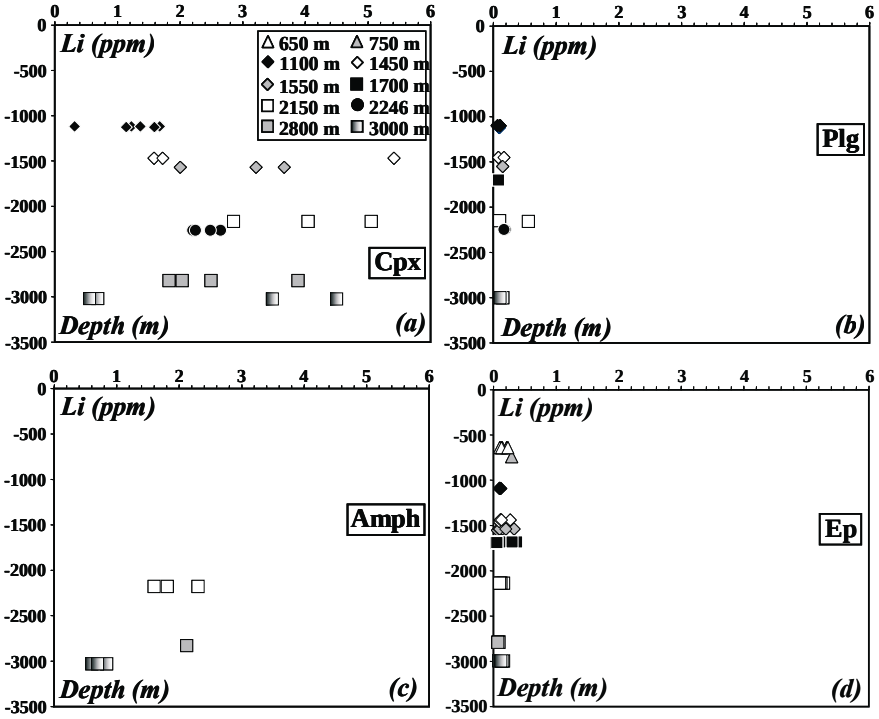

Figure 2. Lithium contents (ppm) versus depth (m) for: (a) clinopyroxene (cpx), (b) plagioclase (plg), (c) amphibole (amph) and (d) epidote (ep).

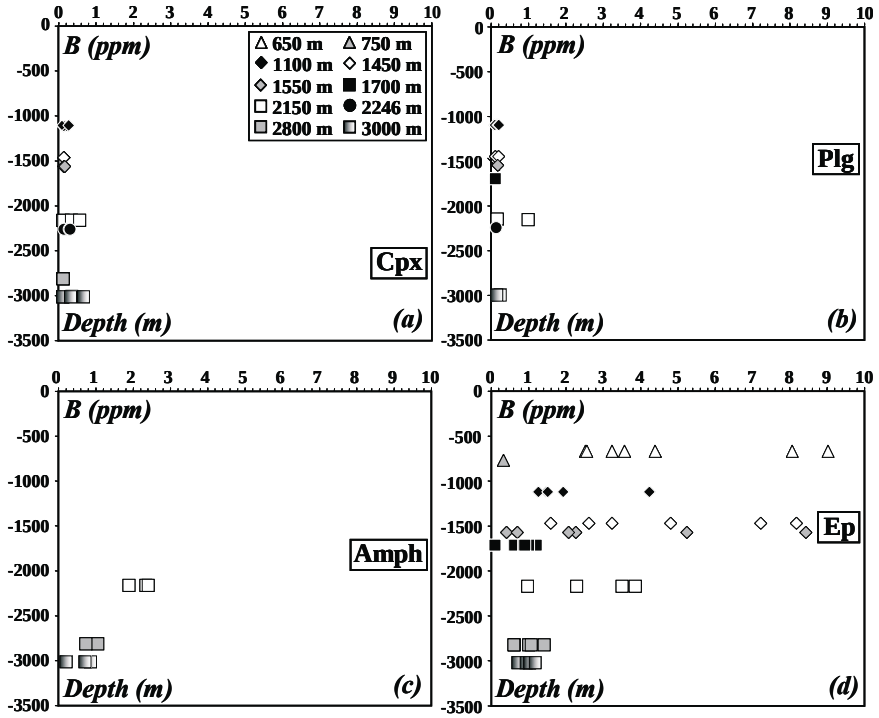

Figure 3. Boron contents (ppm) versus depth (m) for: (a) clinopyroxene (cpx), (b) plagioclase (plg), (c) amphibole (amph) and (d) epidote (ep).

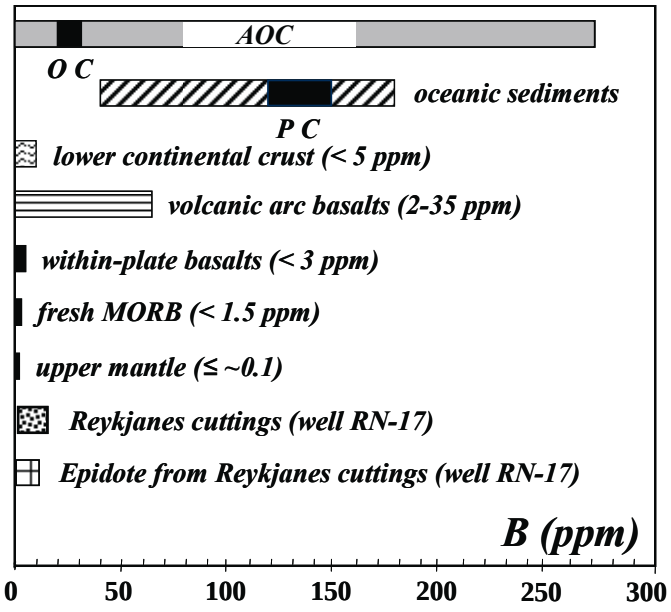

Figure 4. Ranges in boron (B) concentration (ppm) from well RN-17 for epidote (by SIMS) and the overall 11 cuttings determined by ID. Literature B-contents for selected petrologic reservoirs [26] are reported for the purposes of comparison: AOC = altered oceanic crust; OC = oceanic crust; PC = pelagic clay; MORB = mid-ocean ridge basalts.

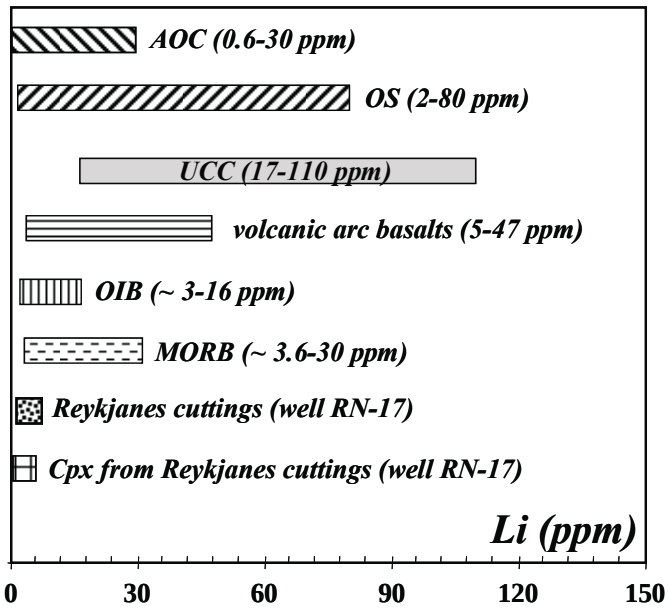

Figure 5. Ranges in lithium (Li) concentration (ppm) from well RN-17 for clinopyroxene (by SIMS) and the overall 11 cuttings determined by ICP-MS. Literature Li-contents for selected petrologic reservoirs [27-31] are reported for the purposes of comparison: AOC = altered oceanic crust; OS = oceanic sediments; UCC = upper continental crust; OIB = ocean island basalts; MORB = mid-ocean ridge basalts.

on the two different major-element compositional areas, however, have not revealed differences in the concentrations of light lithophile and halogen elements.

The high B affinity for epidote places limits on the variation of the alteration degree beneath the Reykjanes system: the increased B-contents in epidote with decreasing depth (figure 3d) suggests, in fact, that the alteration has been more efficient in the shallow and intermediate cuttings than in the deep ones. Moreover, epidote occurrence down to the bottom of the drilled-well (~ 3000 m depth) [1] is also evidence of the persistence of high water/rock interaction at depth. This is in agreement with the results obtained by [6] in the fact that in the Reykjanes geothermal field the density of impermeable intrusive rocks is low between 1 - 2 km depth.

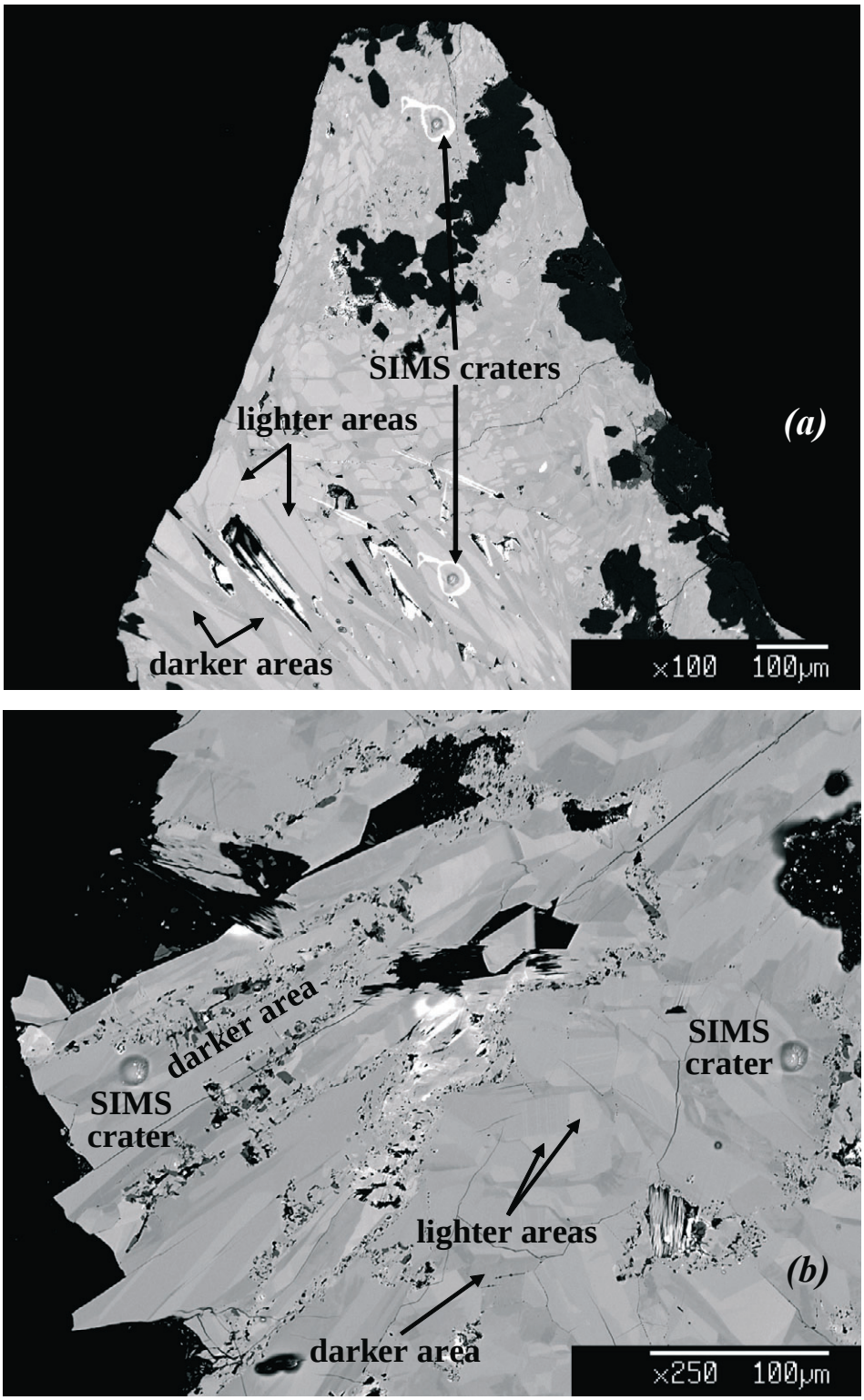

Figure 6. SEM backscattered electron images of epidotes from cuttings RN-17-1100 and RN-17-1700. The micrographs document the occurrence of darker and lighter areas in epidotes, corresponding to different major-element chemical compositions (see text for details). Note the SIMS craters after ion bombardment.

The $\delta^{11}B$ values of the cuttings of the present study, in the range -15.4 ‰ - -4.4 ‰, have been compared with those obtained by [15, 16] on the pristine Icelandic mantle, -10 ± 2 ‰, and with those of fresh glasses, -3.0 ± 0.1 ‰, from the Reykjanes system. The wide negative $\delta^{11}B$ range of our cuttings is a matter of discussion on the nature of the process or processes that occurred in this area. Two scenarios can be invoked: the former could be related to primary characteristics of parental melts; the latter could be ascribed to early interaction with B-poor fluids, like meteoric water, followed by interaction with hydrothermal fluids.

The first hypothesis stems from the fact that most of our cuttings have $\delta^{11}B$ values comparable both with those of ocean island basalts (OIB) ($\delta^{11}B$ = -15 ‰ - 0 ‰; [16-20] and with those of melt inclusions ($\delta^{11}B$ = -13.9 ‰ - -8.2 ‰) in olivine of tholeiitic lavas from the Reykjanes and Hengill volcanic fissure swarms [16] (figure 7), thus suggesting the occurrence of mantle source heterogeneity beneath the Reykjanes area. If this suggestion were valid, the cuttings with the lowest $\delta^{11}B$ values, that is RN-17-1550 ($\delta^{11}B$ = -15.4 ‰) and -3000 ($\delta^{11}B$ = -14.4 ‰), should have OIB affinity. This hypothesis, however, fails for three main reasons at least: 1) B is essentially concentrated in the epidote that is an hydrothermally-related secondary mineral; 2) as documented by [8], whole rock REE patterns (obtained by ICP-MS) of these two samples are different: RN-17-1550 is characterized by REE-contents and fractionations more similar to those of Iceland mildly alkaline lavas than tholeiite ones, whereas RN-17-3000 shows REE-concentrations and fractionations in the range of tholeiite lavas; and 3) no clear correlation is observed between $\delta^{11}B$ and one of the more sensitive parameters of magmatic origin; that is Nd, isotope ratios (figure 8).

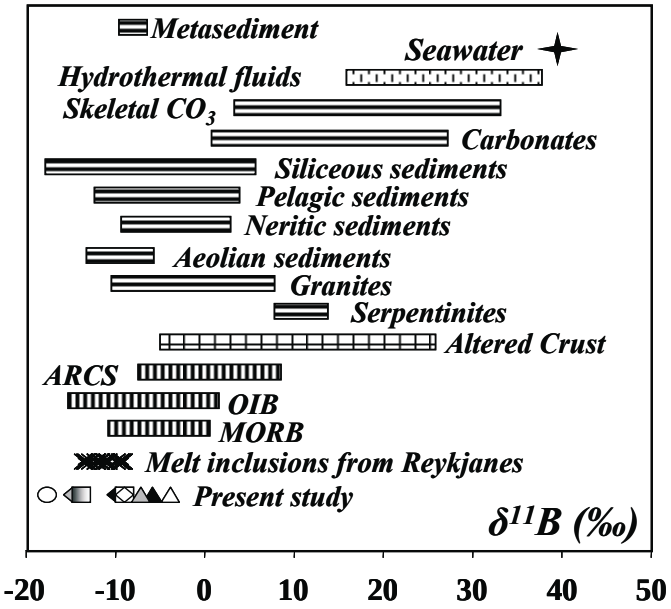

Figure 7. Range of B isotope composition ($\delta^{11}B$) in our cuttings (present study: symbols are those of figures 2 and 3, with the addition of an open circle, for the surface lava RN-17-GIOV-2, and a filled triangle, for the cutting RN-17-400) compared to those of natural reservoirs from literature: ARCS = volcanic arc lavas; OIB = ocean island basalts; MORB = mid-ocean ridge basalts. Data sources are from [26], except for MORB [15, 17, 32, 33] and for melt inclusions from Reykjanes [14].

As far as the second hypothesis is concerned, the interaction with B-poor fluids, like meteoric water, was able to remove B (and particularly ^{11}B) from the rocks as suggested by the $\delta^{11}B$ (-18.3 ± 0.6 ‰) value of the surface lava studied here (RN-17-GIOV-2), which is close to that of travertine deposit ($\delta^{11}B$ = -22 ± 0.5 ‰) from Iceland as reported by [21]. This evidence, along with the fact that GIOV-2 represents the extreme lowest end-member of the positive correlation between $\delta^{11}B$ and Sr isotope ratios (figure 8), leads us to consider that all basaltic rocks from the Reykjanes geothermal field have been affected by an early meteoric water alteration during their magmatic origin. The successive interaction with highly-saline hydrothermal fluids, close to seawater ([22] and references therein), occurring in the Reykjanes system would have progressively enriched in ^{11}B, and

^{87}Sr, the whole drilled rock sequence with decrease of depth. This suggestion seems to be confirmed by studies on the stable isotope composition (δD) of modern geothermal fluids and hydrothermal epidote from the Reykjanes geothermal system by [23, 24]. The authors have observed that, although the chloride concentration of modern Reykjanes geothermal fluids ([22] and references therein) indicates that modern geothermal fluids are hydrothermally-modified seawater, the low measured hydrogen isotope values of these fluids (δD <-23 ‰) and of hydrothermal epidotes (δD = -78 ‰ - -60 ‰) are not in isotopic equilibrium with present-day geothermal fluids but retain an isotopic signature of a glacially-dominated fluid source early in the evolution of the Reykjanes system [24].

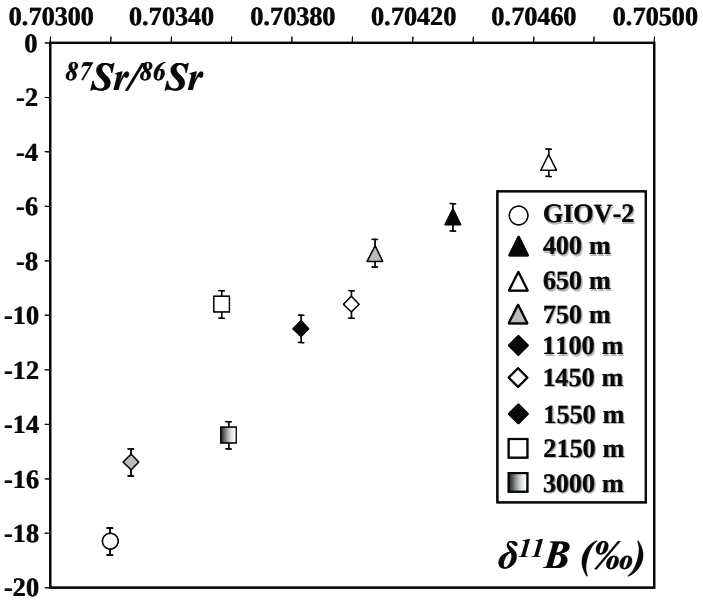

Figure 8. Plot of $^{87}Sr/^{86}Sr$ isotopic ratio versus $\delta^{11}B$ of studied cuttings. The positive correlation indicates an increase of alteration degree with decreasing depth.

6. Conclusion

SIMS investigations of the light lithophile (Li, Be and B) and halogen (F) elements of selected mineral phases of 9 drill-cuttings from the Reykjanes geothermal system have confirmed that epidote, as mineral phase, and B, as trace element, are the main indicators to understand hydrothermal alteration affecting the oceanic crust beneath the Reykjanes area. This alteration has been efficient down to the well-bottom showing the higher degrees in the shallow and intermediate drilled levels.

The positive correlation between whole rock $\delta^{11}B$ and Sr isotope ratios have allowed the alteration to be ascribed to the interaction with hydrothermally-modified seawater. Moreover, the negative whole rock $\delta^{11}B$ values can be accounted for by considering an early interaction with meteoric water, followed by circulation of seawater-hydrothermal fluids. These latter would have re-enriched in ^{11}B all the rock sequences progressively from the bottom to the top of the studied well.

Acknowledgements

This research has been funded to L. Ottolini by CNR grants (year 2008): RSTL: Study of basaltic crust of Iceland (Iceland Deep Drilling Project, IDDP).

References

[1] Fridleifsson G Ó and Elders W A 2007 Progress report on the Iceland Deep Drilling Project (IDDP). *Scientific Drilling* **4**

[2] Fridleifsson G Ó and Albertsson A 2000 *Proceedings World Geothermal Congress 2000*
[3] Raffone N, Ottolini L, Tonarini S, Gianelli G and Fridleifsson G Ó 2008 *Microchim. Acta* **161** 307
[4] Franzson H, Zierenberg R and Schiffman P 2008 *J. Volcanol. Geotherm. Res.* **173** 217
[5] Von Damm K L 1995 *Geophys. Monogr.* **91** 222
[6] Fridleifsson G Ó, Blischkem A, Kristjánsson B R, Richter B, Einarsson G M, Jónasson H, Franzson H, Sigurðsson Ó, Danielsen P E, Jónsson S J, Thordarson S, Thórhallsson S, Harðardóttir H and Egilson Th 2005 *Reykjanes Well Report RN-17 & RN-17ST*
[7] Arnórsson S 1995 *Geothermics* **24** 561
[8] Raffone N, Ottolini L, Tonarini S, D'Orazio M, Gianelli G and Fridleifsson G Ó 2010 Submitted for publication to G-cubed
[9] Tonarini S, Pennisi M, Adorni-Braccesi A, Dini A, Ferrara G, Gonfiantini R, Wiedenbeck M and Gröning M 2003 *J. Geost. Geoanal.* **27** 21
[10] Catanzaro E J, Champion C E, Garner E L, Malinenko G, Sappenfeld K M and Shields W R 1970 *US Natl. Bur. Stand. Spec. Publ.* **260** 17
[11] D'Orazio M 1995 *Per. Min.* **64** 315
[12] Ottolini L, Bottazzi P and Vannucci R 1993 *Anal. Chem.* **65** 1960
[13] Ottolini L, Bottazzi P and Zanetti A 1994 Quantitative analysis of hydrogen, fluorine and chlorine in silicates using energy filtering. *SIMS IX, Proceedings of the 9th International Conference on Secondary Ion Mass Spectrometry* (Benninghoven A, Nihei Y, Shimizu R and Werner H W, eds.) Yokohama (Japan), November 7-12, 1993, (Chichester: John Wiley and Sons) 191
[14] Stecher O 1998 *Geochim. Cosmochim. Acta* **62** 3117
[15] Chaussidon M and Jambon A 1994 *Earth Planet. Sci. Lett.* **121** 277
[16] Gurenko A A and Chaussidon M 1997 *Chem. Geol.* **135** 21
[17] Chaussidon M and Marty B 1995 *Science* **269** 383
[18] Tanaka R and Nakamura E 2005 *Geochim. Cosmochim. Acta* **69** 3385
[19] Tonarini S, Agostini S, Innocenti F and Manetti P 2005 *Terra Nova* **17** 259
[20] Turner S, Tonarini S, Bindeman I, Leeman W P and Schaefer B F 2007 *Nature* **447** 702
[21] Aggarwal J K, Palmer M R, Bullen T D, Arnórsson S and Ragnarsdóttir K V 2000 *Geochim. Cosmochim. Acta* **64** 579
[22] Lonker S W, Frazson H and Kristmannsdóttir H 1993 *Am. J. Sci.* **293** 605
[23] Arnórsson S 1995 *Geothermics* **24** 603
[24] Pope E C, Bird D K, Arnórsson S, Fridriksson T, Elders W A and Fridleifsson G Ó 2008 Am. Geophys. Union, Fall Meeting 2008, abstract #V41B-2070
[25] Hards V L, Kempton P D, Thompson R N and Greenwood P B 2000 *J. Volcanol. Geotherm. Res.* **99** 97
[26] Leeman W P and Sisson V B 1996 Geochemistry of boron and its implications for crustal and mantle processes. *Rev. Mineral.* **33** 645
[27] Ryan J G and Langmuir C H 1987 *Geochim. Cosmochim. Acta* **51** 1727
[28] Tomascak P B, Widom E, Benton L D, Goldstein S L and Ryan J G 2002 *Earth Planet. Sci. Lett.* **196** 227
[29] Leeman W P, Tonarini S, Chan L H and Borg L E 2004 *Chem. Geol.* **212** 101
[30] Bouman C, Elliot T and Vroon P Z 2004 *Chem. Geol.* **212** 59
[31] Teng F-Z, McDonough W F, Rudnick R L, Dalpé C, Tomascak P B, Chappell B W and Gao S 2004 *Geochim. Cosmochim. Acta* **68** 4167
[32] Roy-Barman M, Wasserburg G J, Papanastassiou D A and Chaussidon M 1998 *Earth Planet. Sci. Lett.* **154** 331
[33] Le Roux P J, Shirey S B, Benton L, Hauri E H and Mock T D 2004 *Chem. Geol.* **203** 123